Bach1 derepression is neuroprotective in a mouse model of Parkinson's disease

Manuj Ahuja[a,b,1], Navneet Ammal Kaidery[a,b], Otis C. Attucks[c], Erin McDade[c], Dmitry M. Hushpulian[d], Arsen Gaisin[e], Irina Gaisina[f], Young Hoon Ahn[g], Sergey Nikulin[d], Andrey Poloznikov[d], Irina Gazaryan[d,h,i], Masayuki Yamamoto[j,k], Mitsuyo Matsumoto[l], Kazuhiko Igarashi[l], Sudarshana M. Sharma[m], and Bobby Thomas[a,b,n,o,2]

[a]Darby Children's Research Institute, Medical University of South Carolina, Charleston, SC 29425; [b]Department of Pediatrics, Medical University of South Carolina, Charleston, SC 29425; [c]vTv Therapeutics LLC, High Point, NC 27265; [d]Faculty of Biology and Biotechnology, National Research University Higher School of Economics, Moscow 109028, Russia; [e]Integrated Molecular Structure Education and Research Center, Northwestern University, IL 60208; [f]Department of Pharmaceutical Sciences, College of Pharmacy, University of Illinois, Chicago, IL 60612; [g]Department of Chemistry, Wayne State University, Detroit, MI 48202; [h]Department of Chemical Enzymology, M. V. Lomonosov Moscow State University, Moscow 119991, Russia; [i]Department of Chemistry and Physical Sciences, Pace University, Pleasantville, NY 10570; [j]Department of Medical Biochemistry, Tohoku University Graduate School of Medicine, Sendai 980-8575, Japan; [k]Tohoku Medical Megabank Organization, Tohoku University Graduate School of Medicine, Sendai 980-8573, Japan; [l]Department of Biochemistry, Tohoku University Graduate School of Medicine, Sendai 980-8575, Japan; [m]Department of Biochemistry and Molecular Biology, Hollings Cancer Center, Medical University of South Carolina, Charleston, SC 29425; [n]Department of Neuroscience, Medical University of South Carolina, Charleston, SC 29425; and [o]Department of Drug Discovery, Medical University of South Carolina, Charleston, SC 29425

Edited by Solomon H. Snyder, Johns Hopkins University School of Medicine, Baltimore, MD, and approved September 1, 2021 (received for review July 8, 2021)

Parkinson's disease (PD) is a progressive neurodegenerative movement disorder characterized by the loss of nigrostriatal dopaminergic neurons. Mounting evidence suggests that Nrf2 is a promising target for neuroprotective interventions in PD. However, electrophilic chemical properties of the canonical Nrf2-based drugs cause irreversible alkylation of cysteine residues on cellular proteins resulting in side effects. Bach1 is a known transcriptional repressor of the Nrf2 pathway. We report that Bach1 levels are up-regulated in PD postmortem brains and preclinical models. Bach1 knockout (KO) mice were protected against 1-methyl-4-phenyl-1,2,3,6-tetrahydropyridine (MPTP)-induced dopaminergic neurotoxicity and associated oxidative damage and neuroinflammation. Functional genomic analysis demonstrated that the neuroprotective effects in Bach1 KO mice was due to up-regulation of Bach1-targeted pathways that are associated with both Nrf2-dependent antioxidant response element (ARE) and Nrf2-independent non-ARE genes. Using a proprietary translational technology platform, a drug library screen identified a substituted benzimidazole as a Bach1 inhibitor that was validated as a nonelectrophile. Oral administration of the Bach1 inhibitor attenuated MPTP neurotoxicity in pre- and posttreatment paradigms. Bach1 inhibitor–induced neuroprotection was associated with the up-regulation of Bach1-targeted pathways in concurrence with the results from Bach1 KO mice. Our results suggest that genetic deletion as well as pharmacologic inhibition of Bach1 by a nonelectrophilic inhibitor is a promising therapeutic approach for PD.

Parkinson's disease | MPTP | Nrf2 | Bach1 | transcriptional repressor

Parkinson's disease (PD) is the most common age-related, progressive, neurodegenerative movement disorder characterized by loss of midbrain dopaminergic neurons of the substantia nigra pars compacta (SNpc) (1). PD afflicts more than 10 million people worldwide and is the fastest-growing neurological disorder in terms of prevalence, disability, and deaths, without any cure. [https://www.parkinson.org/ (2–4)]. PD is a multifactorial disease caused by genetic, environmental, and aging-related factors such as elevated oxidative stress, exaggerated inflammation, and abnormalities in cellular metabolic pathways (2). A validated target for PD that could modulate multiple etiological pathways involves drug-induced activation of a coordinated genetic program to maintain redox equilibrium by expressing prosurvival proteins and cytoprotective genes (5). A key transcription factor orchestrating this process is nuclear factor erythroid 2-related factor 2 (Nrf2), a member of the Cap 'n' Collar family of basic leucine zipper transcription factors. Under normal homeostatic conditions, Keap1 (Kelch-like associated protein 1) anchors Nrf2 within the cytoplasm, targeting it for ubiquitination and degradation by the 26S proteasome. In response to oxidative stress or upon exposure to Nrf2 activators, Nrf2 dissociates from Keap1, which prevents Nrf2 ubiquitination and proteasomal degradation (6). Consequently, free Nrf2 translocates to the nucleus, where it dimerizes with Maf proteins (7) and binds the antioxidant response element (ARE), a *cis*-acting enhancer sequence located in the promoter region of a battery of genes. Nrf2 regulates the transcription of over 250 genes, building a multifaceted network that integrates cellular activities [i.e., drug detoxification, immunomodulation, maintenance of both redox and protein homeostasis, and energy metabolism (8)]. The breadth of this

Significance

The Keap1-Nrf2 signaling pathway is a promising therapeutic target for Parkinson's disease (PD). Canonical Nrf2 activators targeting Keap1 thiols are known to be preventive but never effectively cure chronic neurodegeneration because of their electrophilic nature, resulting in nonspecific reactions with active cysteine residues in a variety of cellular proteins. We show that genetic and pharmacologic inhibition of the Nrf2 repressor Bach1 in a posttreatment regimen of experimental PD is neuroprotective by up-regulating Bach1-targeted pathways involving both Nrf2-dependent antioxidant response element (ARE) and non-ARE genes. Inhibition of Bach1 by a nonelectrophilic substituted benzimidazole is a promising therapeutic approach for PD.

Author contributions: M.A., N.A.K., O.C.A., E.M., D.M.H., A.G., I.N.G., S.N., A.P., I.G., S.M.S., and B.T. designed research; M.A., N.A.K., O.C.A., E.M., D.M.H., A.G., I.N.G., S.N., A.P., I.G., and S.S. performed research; Y.-H.A., I.G., M.Y., M.M., and K.I. contributed new reagents/analytic tools; M.A., N.A.K., O.C.A., E.M., D.M.H., A.G., I.N.G., S.N., A.P., M.M., K.I., S.S., and B.T. analyzed data; M.A., N.A.K., and B.T. wrote the paper; M.Y. provided scientific advice for the manuscript; and B.T. supervised the project and acquired funding for the study.

The authors declare no competing interest.

This article is a PNAS Direct Submission.

[1]Present address: Department of Pharmaceutical Sciences, University of Buffalo, Buffalo, NY 14214.

[2]To whom correspondence may be addressed. Email: thomasbo@musc.edu.

This article contains supporting information online at http://www.pnas.org/lookup/suppl/doi:10.1073/pnas.2111643118/-/DCSupplemental.

Published November 5, 2021.

endogenous response suggests that its activation counteracts many of the large numbers of etiological pathways implicated in PD. Complications with pharmacologic activation of Nrf2 to treat neurodegenerative disorders such as PD originate from the electrophilic nature of canonical Nrf2 activators. These electrophiles not only react with cysteines on Keap1 to activate Nrf2 but nonspecifically alkylate cysteine residues on multiple protein targets, leading to side effects (9, 10). The use of existing thiol-modifying agents as inducers of Nrf2 is problematic unless these agents target thiols specific to Keap1 (9, 10). A promising and safe approach to stabilize and activate Nrf2 is to use nonelectrophilic displacement activators targeting the Keap1 Kelch domain and thus dissociating Nrf2 from Keap1 (10). However, despite extensive research in this area, no promising nonelectrophilic displacement activator has been identified as a therapeutic agent for neurodegenerative diseases (9, 10).

BTB and CNC homology 1 (Bach1) is a member of the Cap 'n' Collar and basic region leucine zipper family (CNC-bZIP) of transcription factors. The C-terminal region of Bach1 contains a bZIP domain that binds to DNA by forming heterodimers of Bach1 with small Maf proteins. The Bach1-Maf heterodimers bind to the Maf recognition elements (MAREs) in the promoters of Nrf2 target genes and inhibit transcription (11, 12). Bach1 is ubiquitously expressed in mammalian tissues and is known to regulate various cellular processes [i.e., oxidative stress response, heme homeostasis, cell cycle regulation, cellular differentiation, immunity, adipogenesis, and cellular bioenergetics (13, 14)]. Bach1 ablation is cytoprotective, as it suppresses reactive oxygen species (ROS) generation, mitigates excessive inflammation, improves mitochondrial function, and inhibits apoptosis (13). Multiple studies have demonstrated that Bach1 inhibition/deletion is beneficial in a wide range of disorders, including spinal cord injury (15, 16), atherosclerosis (17), ischemia/reperfusion injury (18), pulmonary fibrosis (19), Huntington's disease (20), experimental autoimmune encephalomyelitis (21), cardiomyopathy (22), cancer (14, 23–25), and in age-related decline in Nrf2 pathway (13). The protective role of Bach1 deletion against neuronal degeneration suggests that Bach1 may represent a promising therapeutic target for neurodegenerative diseases by activating the Nrf2 pathway. In this study, we demonstrated that Bach1 is up-regulated in postmortem PD brains and preclinical disease models. Genetic knockdown of Bach1 in mice protected against 1-methyl-4-phenyl-1,2,3,6-tetrahydropyridine (MPTP) neurotoxicity that was associated with up-regulation of Nrf2-dependent ARE and Nrf2-independent non-ARE pathways. We used a proprietary translational technology platform to identify Bach1 inhibitors, established nonelectrophilic properties of a substituted benzimidazole Bach1 inhibitor, and demonstrated its efficacy against MPTP neurotoxicity in the pre- and posttreatment paradigms. Our results suggest that genetic deletion as well as pharmacologic inhibition of Bach1 by a nonelectrophilic inhibitor is a promising therapeutic strategy for PD.

Results

Bach1 Is Up-regulated in Postmortem Human PD- and Toxin-Based Preclinical Models of PD. Mitochondrial dysfunction, oxidative stress, and neuroinflammatory processes play significant roles in the pathogenesis of PD. Bach1 represses genes that combat oxidative stress, mitochondrial dysfunction, and neuroinflammation (13, 14). To determine if Bach1 expression is affected during nigrostriatal dopaminergic neurodegeneration, we assessed the expression of Bach1 in the brains of sporadic PD patients and toxin-induced preclinical models of PD. Compared to age-matched controls, we observed a significant up-regulation of Bach1 protein levels in the substantia nigra pars compacta (SNpc) of human postmortem PD (Fig. 1 *A* and *B* and *SI Appendix*, Table S1). The parkinsonian neurotoxin MPTP and its toxic metabolite MPP+ cause neurodegeneration by inducing oxidative stress, neuroinflammation, and mitochondrial dysfunction. Time-course analysis of Bach1 expression in the MPTP-treated ventral midbrains (VBMs, the brain region that contains SNpc) in mice showed a significant up-regulation of Bach1 protein levels compared to saline-treated controls. Bach1 levels were significantly up-regulated as early as 2 h after MPTP before the onset of nigrostriatal neurodegeneration. Bach1 levels stayed up-regulated until the seventh day after MPTP, when dopaminergic neuronal cell death is at its peak (Fig. 1 *C* and *D*). Consistent with the MPTP data, time-course analysis following MPP+ (toxic metabolite of MPTP) treatment in N27 rat dopaminergic cells showed a significant up-regulation of Bach1 protein levels at 2 and 8 h compared to controls. By the time peak cell death occurs in the N27 cells at 24 h, Bach1 levels were significantly reduced compared to MPP+ (at 2 and 8 h) and control groups (Fig. 1 *E* and *F*). These data indicate that Bach1 levels are up-regulated in

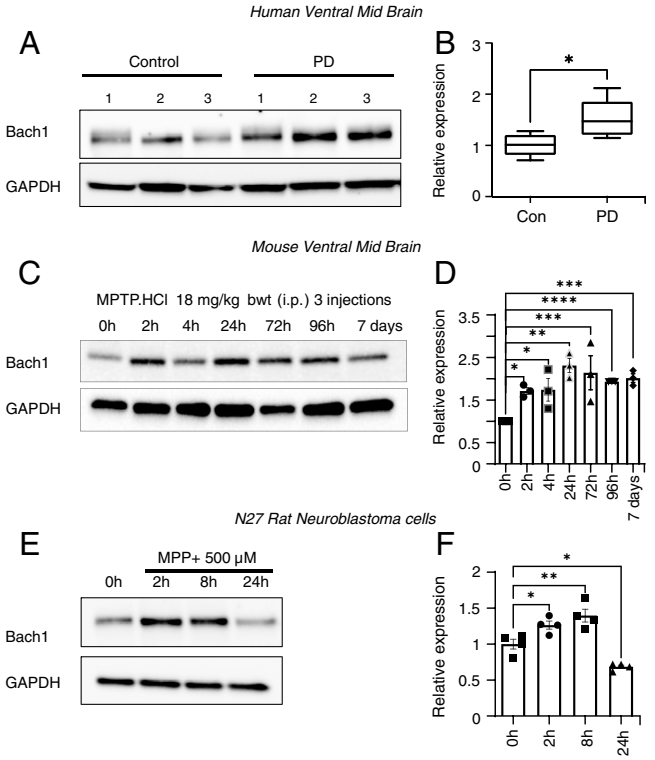

Fig. 1. Bach1 is up-regulated in human postmortem PD brains and in preclinical PD models. (*A*) Immunoblot comparing Bach1 levels in the substantia nigra of age-matched controls and PD patients. (*B*) Quantitative densitometric representation of Bach1 expression after normalization with GAPDH. Data expressed as mean ± SEM ($n = 5$). Statistical analysis used two-tailed unpaired Student's *t* test with $*P < 0.05$ compared to control. (*C*) Immunoblot showing Bach1 levels in the VMB of MPTP-HCl (18 mg/kg, three injections 2 h apart)-treated C57BL/6J mice at different time points (Control, 2 h, 4 h, 24 h, 72 h, 96 h, and 7 d after last MPTP injection). (*D*) Densitometric analysis of Bach1 levels (normalized to GAPDH expression) relative to control. Data expressed as mean ± SEM ($n = 3$). One-way ANOVA with Dunnett's multiple comparison was used to compare between control with other MPTP-treated time points ($*P < 0.05$, $**P < 0.005$ compared to control). (*E*) Time course analysis of Bach1 levels by immunoblot in MPP+ (500 µM)-treated N27 rat dopaminergic cells. (*F*) Densitometric analysis of Bach1 levels (normalized to GAPDH expression) relative to control. Data expressed as mean ± SEM ($n = 3$). One-way ANOVA with Dunnett's multiple comparison was used to compare between control with other time points ($*P < 0.05$, $**P < 0.005$ compared to control). PD, Parkinson's disease; SEM., SE of mean; GAPDH, Glyceraldehyde 3-phosphate dehydrogenase; MPP+, 1-methyl-4-phenylpyridinium; Con, Control.

postmortem human brains and preclinical neurotoxin models of PD, suggesting that increased Bach1 activity may be related to PD pathophysiology.

Ablation of Bach1 Mitigates MPTP-Induced Neurodegeneration. In light of the sporadic PD- and MPTP-induced SNpc Bach1 up-regulation, we asked whether Bach1 levels are implicated in MPTP-induced nigrostriatal dopaminergic neurodegeneration. To test this hypothesis, we compared acute and subacute modes of MPTP neurotoxicity in mutant mice deficient in Bach1 (Bach1 KO) with that of their wild-type (WT) littermates. The mechanism of cell death differs in the acute versus subacute MPTP models, and the latter is more apoptotic compared to nonapoptotic mode of cell death observed in acute MPTP regimen (26). Stereological counts of SNpc dopaminergic neurons defined by tyrosine hydroxylase (TH) and Nissl staining did not differ between WT and Bach1 KO mice after saline injections (Fig. 2 *A*–*D*). SNpc dopaminergic neuronal counts were significantly reduced in WT mice after MPTP injections in the acute (Fig. 2 *A* and *B*) and subacute paradigms (Fig. 2 *C* and *D*). However, in Bach1 KO mice, SNpc dopaminergic neurons were significantly protected against acute (Fig. 2 *A* and *B*) and subacute (Fig. 2 *C* and *D*) paradigms of MPTP neurotoxicity, as more TH- and Nissl- stained SNpc neurons survived in MPTP-treated Bach1 KO mice compared to MPTP-treated WT littermates. In the striatum (STR), MPTP administration in the acute (*SI Appendix*, Fig. S1*A*) and subacute (*SI Appendix*, Fig. S1*B*) paradigms resulted in significant depletion of dopamine (DA) and its metabolites 3,4-dihydroxyphenylacetic acid (DOPAC) and homovanillic acid (HVA) in the WT mice. However, in Bach1 KO mice, MPTP-induced loss of DA and its metabolites in the acute (*SI Appendix*, Fig. S1*A*) and subacute (*SI Appendix*, Fig. S1*B*) paradigms were significantly attenuated compared to MPTP-injected WT mice. These findings demonstrate the crucial role of Bach1 in mediating neurotoxic effects in SNpc dopaminergic neurons.

One of the rate-limiting factors in MPTP neurotoxicity is the conversion of MPTP to MPP+ in the brain. To ascertain that resistance to the neurotoxic effects of MPTP provided by Bach1 ablation was not because of alteration in the bioavailability of MPP+, we measured striatal levels of MPP+ 90 min after MPTP injection. The MPP+ levels did not differ between MPTP-injected Bach1 KO mice compared to WT mice (*SI Appendix*, Table S2). These findings suggest that attenuation of MPTP-neurotoxicity in Bach1 KO mice was not due to alterations in conversion of MPTP to MPP+ in the brain.

Pathway Analysis Reveals that Bach1 Ablation Induces Both ARE- and Non–ARE-Mediated Neuroprotective Pathways

To evaluate the effect of Bach1 ablation in mouse VMB, total RNA from the VMB of 2-mo-old mice was subjected to a whole-genome gene expression analysis using the Affymetrix platform (see *Materials and Methods*). Microarray data demonstrated that 1,164 genes were differentially expressed by more than 1.5-fold compared to WT, with a *P* value cutoff of 0.05 between WT and Bach1 KO VMB samples (Fig. 3*A* and *SI Appendix*, Fig. S2*A* and Table S3). The bioinformatics pipeline used for evaluating differential expression of Bach1 associated genes is described in the scheme (Fig. 3*B*). We utilized a publicly available Bach1 chromatin immunoprecipitation sequencing (ChIP-seq) data (GSM2086721) (27) to identify physical Bach1 association with gene loci. Motif analysis of Bach1 ChIP-seq data identified ∼33% of the Bach1 peaks harboring classical ARE motifs (TGA(G/C)TC) followed by erythroblast transformation specific (ETS) binding motif as the second most abundant motif (18 to 23%) (Fig. 3*C*). Dependent on whether a peak has an ARE motif–bound region, we classified the peak as either a Bach1-ARE or Bach1-non-ARE. The obtained Bach1-ARE and Bach1-non-ARE gene signatures were used to evaluate the enrichment of gene sets using gene set enrichment analysis [GSEA (28)]. Of the 2,242 genes that were associated with Bach1-bound loci as judged by the nearest-neighbor analysis, 48% had ARE elements within the Bach1-bound region, and 52% of genes had non-ARE motifs. About 7% of genes had at least one ARE and one non–ARE-bound Bach1 loci associated with them (Fig. 3*D*). GSEA demonstrated that ARE-associated genes were predominantly enriched for the pathways that were involved in oxygen sensing/regulation/as well as neuronal death (Fig. 3 *E*, *Top* and *SI Appendix*, Fig. S2*B* and Table S4), whereas non–ARE-bound genes mostly accounted for transcription factor binding as well as the neuronal death (Fig. 3 *E*, *Bottom* and *SI Appendix*, Fig. S2*C* and Table S4). A subset of genes enriched in both Bach1 ARE loci (Fig. 3 *E*, *Top* and *SI Appendix*, Table S5) and Bach1 non-ARE loci (Fig. 3 *E*, *Bottom* and *SI Appendix*, Table S5) were validated using RT-PCR from WT and Bach1 KO mice VMB (Fig. 3*F*). These data suggest that Bach1 ablation activates both ARE- and non–ARE-mediated neuroprotective pathways.

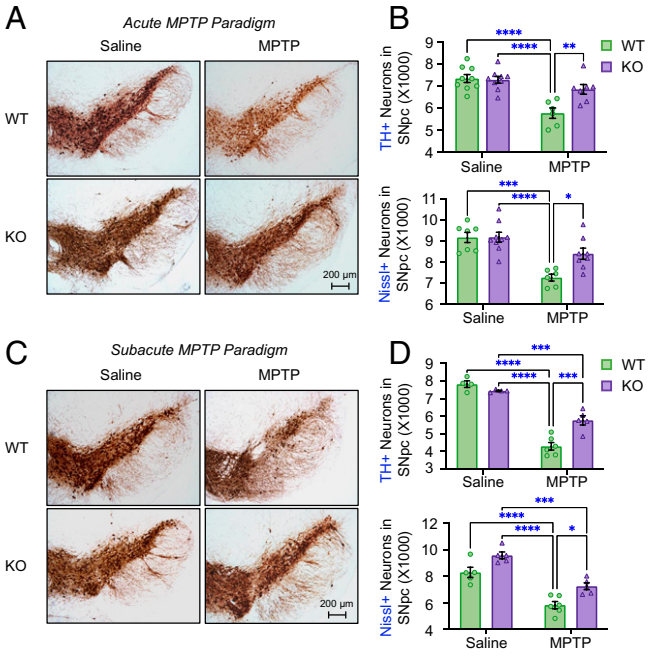

Fig. 2. Bach1 ablation protects against acute and subacute models of MPTP neurotoxicity. (*A*) Immunohistochemical staining for TH and (*B*) stereological analysis of total (Nissl) and TH+ neurons in the SNpc in WT and Bach1 KO (KO) mice on seventh day after acute MPTP (MPTP.HCl 12 mg/kg three injections 2 h apart). Data expressed as mean ± SEM. Two-way ANOVA with Tukey's multiple comparison was used to compare between means of all the groups (*$P < 0.05$, **$P < 0.005$, ***$P < 0.0005$, and ****$P < 0.0001$ compared to the selected group; $n = 6$ to 10 mice per group). (*C*) Immunohistochemical staining for TH and (*D*) stereological analysis of total (Nissl) and TH+ neurons in the SNpc of WT and Bach1 KO (KO) mice performed 14 d after last dose of MPTP in the subacute model (MPTP HCl 36 mg/kg once daily for 5 d). Bars represent mean ± SEM. Two-way ANOVA with Tukey's multiple comparison was used to compare between means of all the groups (*$P < 0.05$, ***$P < 0.0005$, and ****$P < 0.0001$ compared to the selected group; $n = 4$ to 6 mice per group). (Scale bar, 200 μm.) SNpc, substantia nigra pars compacta; TH, tyrosine hydroxylase.

Ablation of Bach1 Attenuates MPTP-Induced Oxidative Stress and Neuroinflammation. Dopaminergic neuronal degeneration in PD and MPTP neurotoxicity is triggered by events that can lead to progressive neuroinflammation and oxidative stress (29, 30).

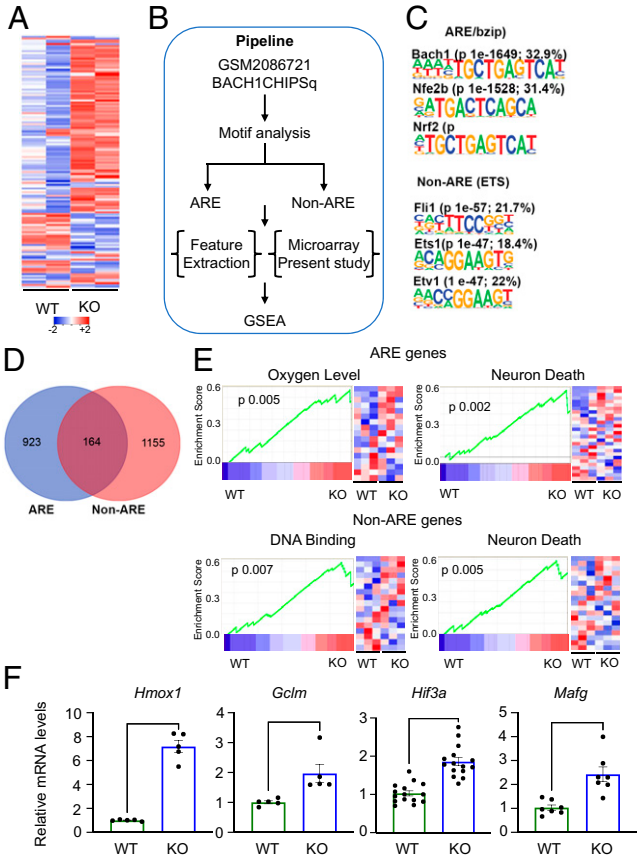

Fig. 3. Bach1 ablation activates Nrf2-dependent ARE and Nrf2-independent non-ARE neuroprotective pathways. (*A*) Heatmap of 1.5-fold differentially expressed genes in the VMB of Bach1 KO (KO) mice compared to WT. (*B*) Schematic representation of the pipeline used for GSEA. (*C*) The highly enriched motifs in the Bach1 peaks (GSM2086721). (*D*) Venn diagram depicting the genes that are associated either with an ARE motif in Bach1 peak or non-ARE motifs in Bach1 peak. (*E*) GSEA of genes that harbors at least one ARE motif from WT and Bach1 KO gene expression data (*Top*). GSEA of genes that harbors at least one non-ARE motif from WT and Bach1 KO gene expression data (*Bottom*). (F) Validation of differentially expressed genes *Hmox1* (ARE and non-ARE gene), *Gclm* (ARE gene), *Hif3a* (non-ARE gene), and *Mafg* (ARE gene) represented in the leading edge of the gene sets associated with enrichment terms in *D* by WT and Bach1 KO mice VMB by qRT-PCR. Bars represent fold expression relative to control values depicted as mean ± SEM. Two-tailed unpaired Student's *t* test was used to compare between WT and KO, $*P < 0.05$, $**P < 0.005$, and $****P < 0.0001$ compared to the WT ($n = 5$ to 15).

Based on our data from the pathway analysis in Bach1 KO VMB, we hypothesized that Bach1 ablation would derepress genes involved in cellular antioxidant transcriptional machinery and induce expression of anti-inflammatory genes. To investigate whether such a mechanism was in play there, we evaluated markers of oxidative stress (3-nitrotyrosine) and reactive glia (CD68, a microglial marker, and glial fibrillary acidic protein [GFAP], an astrocytic marker) as markers for inflammation in the SNpc. Immunohistochemical analysis showed a significant increase in 3-NT immunoreactivity in the MPTP-injected WT mice compared to saline-injected mice (*SI Appendix*, Fig. S3*A*). Bach1 ablation significantly attenuated the MPTP-induced increase in 3-NT immunoreactivity compared to WT mice injected with MPTP both visually (*SI Appendix*, Fig. S3*A*) and quantitatively (*SI Appendix*, Fig. S3*B*). Similarly, MPTP administration significantly increased the CD68-immunopositive activated microglia (*SI Appendix*, Fig. S3*C*) and GFAP-immunopositive reactive astrocytes (*SI Appendix*, Fig. S3*E*) in WT mice compared to saline-injected mice. Bach1 ablation significantly attenuated levels of MPTP-induced reactive microglia and astrocytes compared with MPTP-treated WT mice. Morphometric analysis of CD68-positive reactive microglia and GFAP-positive reactive astrocytes in the SNpc showed a profound increase in the levels of reactive microglial and astrocytic cell counts in the MPTP-treated WT mice compared with saline-injected controls, which were markedly reduced in Bach1 KO mice treated with MPTP (*SI Appendix*, Fig. S3 *D* and *F*). Consistent with the immunohistochemical markers of oxidative stress and neuroinflammation in the SNpc, messenger RNA (mRNA) analysis in the VMB and STR of saline-injected WT and Bach1 KO mice demonstrated a significant increase in the levels of antioxidant and anti-inflammatory genes hemeoxygenase 1 (*Hmox1*) and the modulatory subunit of glutathione cysteine ligase (*Gclm*) (*SI Appendix*, Fig. S4). Administration of MPTP in the WT mice had no significant impact on mRNA levels of *Hmox1* and *Gclm* in the VMB and STR compared to saline-injected WT mice. The mRNA levels of *Hmox1* and *Gclm* showed a significant up-regulation in MPTP-injected Bach1 KO mice when compared with MPTP-treated WT mice (*SI Appendix*, Fig. S4). These findings suggest that neuroprotective effects in Bach1 KO mice against MPTP neurotoxicity is mediated by up-regulation of antioxidant and anti-inflammatory genes and associated with marked reduction in markers of oxidative stress and inflammation.

Substituted Benzimidazole HPPE Is a Nonelectrophilic Bach1 Inhibitor. Based on our findings that Bach1 ablation in mice protected against MPTP-neurotoxicity, Bach1 can be considered a validated target for MPTP-induced PD. To pharmacologically manipulate Bach1, we used a proprietary translational technology platform developed by vTv Therapeutics to identify Bach1 inhibitors (WO 2012/094580) (31). A series of substituted benzimidazole hits were identified as Bach1 inhibitors, which were further validated using a MARE-luciferase reporter assay (see the assay principle in Fig. 4*A*) (31–33). Maf recognition element or MARE are present in the regulatory region of a variety of genes. Bach1 heterodimerizes with small Maf proteins to bind to the MARE elements to repress the expression of MARE-regulated genes. The MARE-luciferase assay picks pharmacophores that work both via Nrf2 activation and Bach1 inhibition. In the MARE-Luciferase assay, the potency of the best hit, *N*-(2-(2-hydroxyethoxy)ethyl)-1-methyl-2-((6-(trifluoromethyl)benzo[*d*]thiazol-2-yl)amino)-1*H*-benzo[*d*]imidazole-5-carboxamide, designated as HPPE (Fig. 4*B* and *SI Appendix*, Fig. S5*A*), was superior to an established physiological Bach1 inhibitor, hemin, and the Food and Drug Administration (FDA)-approved Nrf2 activator, dimethylfumarate (DMF) (Fig. 4*B*). The MARE-luciferase reporter activation by Bach1 inhibitors like cobalt protoporphyrin (Co-PPIX) (34), HPPE, as well as bardoxolone methyl (CDDO-Me) was competitively inhibited by the overexpressed WT Bach1 (Fig. 4*C*). However, the reporter activation observed for Co-PPIX and HPPE was almost completely lost, with the overexpressed Bach1 mutant containing alanine residues in place of cysteines in the CP (cysteine-proline) motifs in the bZIP domain of the Bach1, known for its heme-binding propensity (Fig. 4*C*) (31, 33), whereas activation induced by bardoxolone methyl was insensitive to the presence of the mutant Bach1. The absence of activation by Bach1 inhibitor Co-PPIX and potential inhibitor HPPE in the presence of the mutant Bach1 confirms that they work by Bach1 displacement mechanism, which occurs via the compound's interaction with the mutated cysteine residues in the CP motifs. Once these cysteine residues are replaced by alanine, both Co-PPIX and HPPE lose their ability to interact with Bach1 and displace it from MARE. Thus, HPPE behaves the same way as Co-PPIX, a known inhibitor of Bach1 and can be considered as a direct Bach1 inhibitor. Based on the HPPE

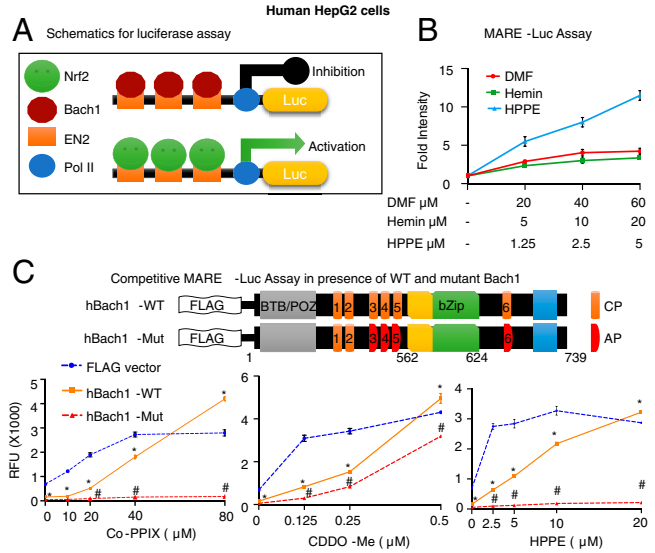

Fig. 4. Bach1 inhibitor HPPE derepress Bach1-mediated repression. (*A*) Schematic representation of the luciferase assay used for validation of derepression mediated by Bach1 inhibition. (*B*) MARE-luciferase activity assay in the presence of increasing concentrations of DMF, Hemin, and HPPE in HepG2 cells 24 h posttransfection. Line graph represents the change in fold intensity of luciferase activity mean ± SEM over controls ($n = 6$). (*C*) Schematic representation of the human Bach1- WT and human Bach1-Mut (alanine substituted at cysteine, AP3-6) expressed in the FLAG vector (*Top*). MARE-luciferase activity assay following overexpression of FLAG vector, hBach1-WT, and hBach1-Mut measured after treatment with Co-PPIX, CDDO-Me, and HPPE for 18 h. Line graph represents the relative fluorescence unit of luciferase activity mean ± SEM. Two-way ANOVA with Bonferroni's multiple comparison was used for comparing the effect of hBach1-WT overexpression with hBach1-Mut at respective concentrations of each compound when compared to the FLAG vector (*$P < 0.05$ compared to FLAG-vector and #$P < 0.05$ compared to hBach1-WT; $n = 6$). DMF, dimethylfumarate; E, HPPE; Co-PPIX, Cobalt Protoporphyrin; CDDO-me, Bardoxolone Methyl; CP, cysteine-proline motif; AP, alanine-proline motif.

chemical structure, which matches one-half of the porphyrin ring (with nitrogen atoms in HPPE benzothiazole and benzimidazole moieties coinciding with nitrogen atoms in two adjacent pyrrole moieties in heme porphyrin ring) (*SI Appendix*, Fig. S5*A*), one may expect HPPE binding to protein sites accommodating metal-porphyrins such as heme itself or Co-PPIX. Since Bach1 has regulatory heme-binding sites, HPPE's ability to bind to the heme-binding sites can be predicted based on the structural considerations.

To determine the specificity of HPPE in activating Bach1 target genes, WT and Bach1 KO immortalized mouse embryonic fibroblasts (iMEFs) were treated with HPPE or hemin. At basal conditions, *Hmox1* was significantly up-regulated in Bach1 KO iMEF compared to WT controls. Both HPPE and hemin significantly up-regulated *Hmox1* mRNA levels in the WT iMEFs compared to vehicle controls (*SI Appendix*, Fig. S6*A*). In contrast, HPPE and hemin treatment in Bach1 KO iMEFs did not exhibit significant up-regulation of *Hmox1* mRNA levels compared to vehicle-treated Bach1 KO iMEFs, (*SI Appendix*, Fig. S6*A*). These results suggest that both HPPE and hemin require functional Bach1 to up-regulate *Hmox1*. To further corroborate our in vitro observations, we administered HPPE in WT and Bach1 KO mice and measured *Hmox1* mRNA levels in the thymus (an organ with the highest Bach1 expression). Consistent with our in vitro findings, the level of *Hmox1* mRNA was significantly elevated in vehicle-treated Bach1 KO thymus compared to WT controls. Administration of HPPE significantly increased *Hmox1* mRNA levels in WT thymus compared to vehicle-treated WT mice. However, HPPE failed to induce a significant up-regulation of *Hmox1* in Bach1 KO thymus compared to thymus from vehicle-treated Bach1 KO mice (*SI Appendix*, Fig. S6*B*). The lack of synergistic induction of *Hmox1* mRNA in Bach1 KO thymus in the presence of HPPE further implies that HPPE-induced up-regulation of *Hmox1* mRNA is mediated by Bach1 inhibition in vivo.

To test the possibility of HPPE covalently binding to Bach1, we performed mass spectrometry analysis for detecting HPPE-modified recombinant Bach1. DMF, a known Nrf2 activator that works via alkylation mechanism and as such, capable of nonspecific alkylation of thiols on cellular proteins, was used as a positive control for the alkylation reaction. The study confirmed that DMF covalently modifies Bach1 cysteines resulting in 2-dimethyl-succinyl modification of Bach1 peptides compared to controls, whereas HPPE failed to covalently modify any of the Bach1 cysteines (*SI Appendix*, Table S6). The confirmed absence of Bach1 alkylation and structural similarity between HPPE and porphyrin supports HPPE classification as a true nonelectrophilic Bach1 inhibitor working via heme-binding sites of the Bach1 protein.

HPPE-Induced Bach1 Derepression Requires Nuclear Export of Bach1. Bach1 inhibitors such as cadmium and hemin induce the Crm1-dependent nuclear Bach1 export, thus modulating nucleocytoplasmic shuttling of Bach1, leading to transcription of Bach1 target genes (35, 36). Hemin is also known to inhibit Bach1 DNA binding and functions through multiple mechanisms to inactivate the repressive effect of Bach1 (32). HPPE treatment significantly up-regulated Hmox1 (a Bach1 target) protein levels, but pretreatment with nuclear export inhibitor Leptomycin B (LeptB) significantly reduced the HPPE-mediated induction of Hmox1 protein levels (Fig. 5 *A* and *B*). Analysis of subcellular fractions after 1 h treatment of neuroblastoma cells showed that there was no change in the total Bach1 levels upon HPPE treatment. However, Bach1 distribution between the nuclear and cytosolic fractions changed, such that the Bach1 protein levels in the nucleus were reduced, whereas its cytosolic levels were increased as compared to the levels of Bach1 in the controls without HPPE treatment, which is consistent with HPPE-induced Bach1 exit to the cytosol (Fig. 5*C*). Pretreatment with LeptB did not change the total Bach1 levels as well but clearly prevented HPPE-mediated Bach1 exit from the nucleus (Fig. 5*C*). The immunoblot also showed accumulation of Nrf2 protein in the cytosol and especially in the nucleus after HPPE treatment, confirming that HPPE exhibited Nrf2 stabilization activity. However, accumulation of Nrf2 in the nucleus by HPPE treatment in the presence of Bach1 export inhibitor LeptB did not up-regulate Hmox1 (Fig. 5 *A* and *B*). This observation makes a strong point in justifying the need for Bach1 inhibition in addition to Nrf2 stabilization to trigger Nrf2-induced genetic program. Apparently, the newly identified Bach1 inhibitor HPPE does both (i.e., stabilizes Nrf2 and mediates Bach1 nucleocytoplasmic shuttling).

To demonstrate the direct effect of HPPE on Bach1 DNA binding and competition between Bach1 and Nrf2 for DNA binding, we measured Bach1 and Nrf2 relative occupancy on the two MARE enhancer regions (EN1, −2 kilobase pair [kbp] and EN2, −9 kbp from the transcription site) on the Hmox1 promoter for HPPE, hemin, a physiological Bach1 inhibitor, and DMF, an alkylating Nrf2 activator. ChIP assay showed that under basal conditions, Bach1 occupancy on EN1 (*SI Appendix*, Fig. S7) and EN2 sites (Fig. 5*D*) was significantly higher than Nrf2 (Fig. 5*E*), pointing to Bach1-mediated repression in the basal resting state. Following HPPE treatment, Nrf2 binding to both EN2 (Fig. 5*E*) and EN1 (*SI Appendix*, Fig. S7) sites was ca. eightfold higher, whereas Nrf2 binding with hemin to EN2 and EN1 sites was ca. fivefold higher compared to controls. This observation may indirectly prove that HPPE has an

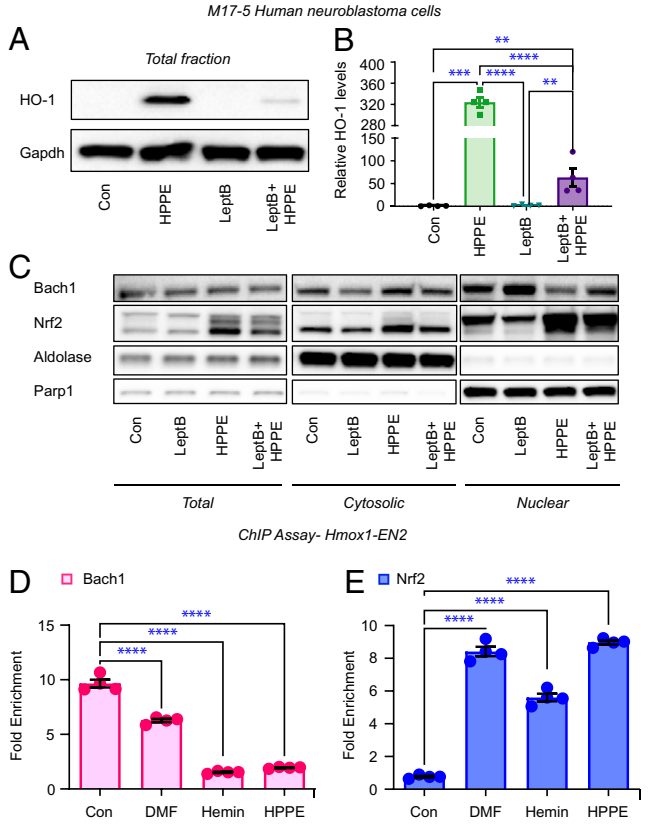

Fig. 5. Nuclear export of Bach1 is required for HPPE-mediated Bach1 derepression. (*A*) Immunoblot and (*B*) densitometric analysis of HO-1 1 h following HPPE (3 μM) or dimethyl sulfoxide (DMSO) (Con) treatment in M17-5 neuroblastoma cells pretreated with either vehicle (0.1% ethanol containing media) or Leptomycin B (LeptB, 20 ng/mL, prepared in 0.1% ethanol containing media) for 1 h normalized to Gapdh. Bars represent percent increase relative to control values expressed as mean ± SEM. One-way ANOVA followed by Tukey's multiple comparison test was used to compare between control and other groups (**$P < 0.005$ and ****$P < 0.0001$; $n = 3$). (*C*) Immunoblot showing total, cytosolic, and nuclear Bach1 and Nrf2 levels in M17-5 neuroblastoma cells. M17-5 neuroblastoma cells were treated as in *A*, and cells were subjected to immunoblot 1 h after HPPE. Aldolase and Parp1 were used to verify the purity of cytosolic and nuclear fractions, respectively. Chromatin immunoprecipitation assay showing the levels of Bach1 (*D*) and Nrf2 (*E*) on Hmox1-EN2 enhancer in M17-5 neuroblastoma cells treated with DMF (20 μM), Hemin (20 μM), and HPPE (5 μM) for 5 h. Bar diagram represents mean ± SEM of fold enrichment of transcription factors. One-way ANOVA with Tukey's multiple comparison was used to compare control with other groups (****$P < 0.0001$; $n = 4$).

additional activity in Nrf2 stabilization besides Bach1 inhibition. The level of bound Nrf2 in the case of HPPE was close to that of DMF, a canonical Nrf2 activator. However, DMF was capable of displacing only one-half of the Bach1 occupied sites (Fig. 5*D*), which is likely a result of nonspecific alkylation of Bach1 cysteines by DMF as we demonstrated previously (37) (*SI Appendix*, Table S6). It is important to note that twofold reduction in Bach1 occupancy does not match the increase in Nrf2 occupancy in the case of DMF treatment, whereas for HPPE and hemin, the Nrf2 binding to both EN2 and EN1 sites were accompanied by a corresponding reduction in Bach1 occupancy compared to control (Fig. 5*D*). These results demonstrate that HPPE combines both activities (e.g., Nrf2 stabilization and Bach1 inhibition in one molecule). HPPE behaves closely to hemin but is fourfold more potent based on the concentrations used to generate a similar response.

In summary, the results of HPPE evaluation with respect to its mechanism of action confirm its nonalkylating nature and specificity for Bach1 derepression, similar to that of the physiological Bach1 inhibitor, hemin. The difference between the two is that the Bach1 inhibitor HPPE is much more potent and will not exert harmful oxidative effects originating from the well-known catalytic properties of hemin.

HPPE Does Not Alkylate Keap1 or Displace Nrf2. HPPE is a direct stabilizer of Nrf2 as judged by its activation (*SI Appendix*, Fig. S8) of Neh2-luciferase reporter specific for Nrf2 stabilizers working via disruption of Keap1-Nrf2 interaction (37). There are two well-characterized mechanisms of Nrf2 stabilization, either by targeting Keap1 thiols or noncovalently displacing Neh2-domain of Nrf2 from its complex with Keap1 through its C-terminal Kelch domains that binds Nrf2 (9). To rule out the possibility of HPPE acting as an alkylating agent targeting Keap1 thiols, we tested the ability of HPPE to covalently modify glutathione (GSH). A simple assay of incubating GSH with either HPPE or DMF was carried out in a test tube as reported previously (37). In accord with our earlier findings, DMF exhibited strong reactivity toward GSH as measured by the amount of GSH consumed by DMF and the corresponding increase in the GS-DMF adducts (Fig. 6 *A* and *B*). However, HPPE showed no reactivity toward GSH as demonstrated by the absence of thiol adducts and preservation of GSH levels (Fig. 6 *A* and *B*). To compare the pro-oxidant potential of HPPE and DMF in vitro, N27 rat dopaminergic cells were treated with either HPPE or DMF to study the changes in the total GSH and ROS levels. Consistent with its electrophilic properties (37), DMF increased ROS and significantly depleted the total GSH content in a dose-dependent manner, whereas HPPE treatment did not increase ROS levels and deplete cellular GSH but instead increased GSH content at 10-μM dose when compared to DMF and vehicle controls (Fig. 6 *C* and *D*).

To evaluate the toxicity of HPPE for humans, we used a liver-on-a-chip device with differentiated HepaRG spheroids with varied concentration of HPPE circulating for 48 h (*SI Appendix*, Fig. S9). The onset of toxicity is observed at 50 μM, which is more than an order of magnitude higher than the concentration of HPPE used to achieve maximum activation effect in the in vitro assays using human cells (Fig. 5).

A distinguishing feature of electrophilic molecules is their inability to activate ARE-luciferase reporters in the presence of reducing agents working as ROS scavengers (37). DMF-induced activation of ARE-luciferase reporter was markedly quenched in the presence of N-acetylcysteine (NAC) and GSH, whereas incubation of NAC or GSH with HPPE failed to quench the ARE-luciferase reporter activity (Fig. 6 *E* and *F*). The same effect was observed using Neh2-luc reporter cells (*SI Appendix*, Fig. S8 *A* and *B*). Finally, we tested if HPPE treatment could modify Keap1 cysteines. Contrary to the previously reported covalent modification of the cysteine residue 151 of the Keap1 protein after DMF treatment (38, 39), HPPE treatment failed to modify Keap1 cysteines (*SI Appendix*, Fig. S10*A*) and impact cellular Keap1 protein levels (*SI Appendix*, Fig. S11). To confirm the mass-spectrometry results, we used Keap1 null mouse embryonic fibroblast that has been modified through CRISPR/Cas9-directed mutagenesis, where cysteine was replaced by serine at position 151 on Keap1 ($Keap1^{C151S/C151S}$) as exemplified by schematics (*SI Appendix*, Fig. S10*C*). In $Keap1^{WT/WT}$ cells, DMF treatment significantly increased *Hmox1* mRNA levels compared to controls, whereas in $Keap1^{C151S/C151S}$ cells, DMF failed to induce *Hmox1* mRNA levels (*SI Appendix*, Fig. S10*B*). In the case of HPPE, *Hmox1* mRNA levels were significantly up-regulated both in $Keap1^{WT/WT}$ and in $Keap1^{C151S/C151S}$ cells, which suggests that HPPE does not require covalent modification of Keap1 cysteine 151 to activate the Nrf2 pathway. Collectively, these results strongly support a nonelectrophilic nature of HPPE.

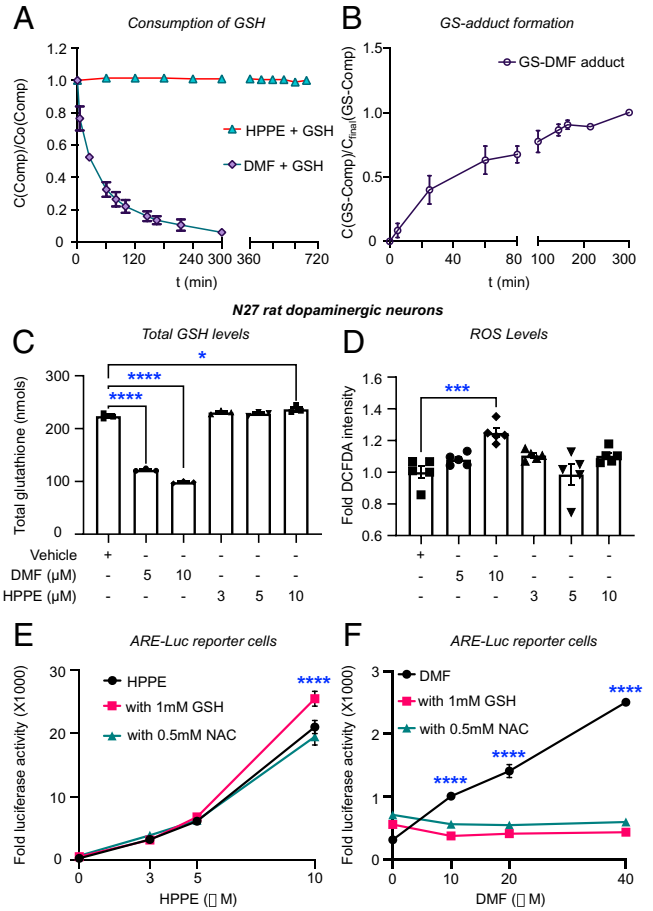

Fig. 6. HPPE is a nonelectrophile. (*A*) Time course of the S-alkylation reaction between 1 mM DMF or 1 mM HPPE with 1 mM GSH in phosphate-buffered saline at pH 7.4 was measured and displayed as (*A*) time course for GSH consumption and (*B*) GS-DMF adduct formation. (*C*) Intracellular total GSH levels were determined at 4 h following DMF (5 and 10 μM) or HPPE (3, 5, and 10 μM) treatment in N27 rat dopaminergic cells. Data expressed as mean ± SEM. One-way ANOVA followed by Dunnett's multiple comparison was used for evaluating statistical significance compared to control group (*$P < 0.05$ or ****$P < 0.0001$; $n = 6$). (*D*) Total ROS levels in N27 rat dopaminergic cells treated with DMF (5 and 10 μM) or HPPE (3, 5, and 10 μM) for 1 h. Bar plot represents the fold intensities relative to control and expressed as mean ± SEM. One-way ANOVA followed by Dunnett's multiple comparison was used for evaluating statistical significance compared to control group (***$P < 0.0005$; $n = 5$). Quenching of the ARE-luciferase reporter activity in the presence of thiol reagents is as follows: 0.5 mM NAC or GSH when treated with (*E*) HPPE and (*F*) DMF for 24 h. Line plot represents fold luciferase activity and expressed as mean ± SEM. Two-way ANOVA with Tukey's multiple comparison test was used to compare HPPE or DMF with thiol reagents (****$P < 0.0001$; $n = 4$). DMF, Dimethyl fumarate; GSH, reduced glutathione.

These experiments establish that HPPE does not interfere with Keap1-Nrf2 binding as a canonical electrophilic Nrf2 activator; however, they do not exclude the possibility that HPPE might act as a displacement activator of Keap1-Nrf2 pathway. A Nrf2-displacement activator is defined as a small molecule/peptide that activates Nrf2 by displacing Nrf2 protein from the Keap1-Nrf2 complex via binding with high affinity to the ETGE-recognition site at Keap1, without covalent modification of Keap1 cysteines (9, 10). To evaluate the probability for HPPE binding in the same site of Kelch domain as for Nrf2 displacement activators, HPPE docking was performed using the known crystal structure of Keap1 Kelch domain with the bound displacement activator Cpd16 (4IQK.pdb). Based on the similar values of CDOCKER interaction energy for Cpd16 (used as control) and HPPE (−46.23 and −47.12 kcal/mol, respectively), one could speculate on the possibility for HPPE to behave as a displacement activator in low micromolar range, like Cpd16 does (*SI Appendix*, Fig. S12). To exclude the possibility for HPPE to act as a displacement activator of Keap1-Nrf2 pathway, we utilized a direct fluorescence polarization assay monitoring the competition between fluorescently labeled Nrf2 peptide and HPPE for Kelch domain binding. HPPE in the concentration range up to 1 mM did not interfere with Keap1-Nrf2 peptide interaction and thus did not change the percentage of fluorescent Nrf2 peptide–bound Keap1. This was in contrast to the unlabeled Nrf2 peptide (peptide 70042) or small molecule displacement activators (SML0959 and CPUY192018) that dose dependently reduced the fluorescent Nrf2 peptide bound Keap1 (*SI Appendix*, Fig. S10*D*).

Collectively, these observations confirm that HPPE is not an electrophile or a displacement activator, but it does stabilize Nrf2 via Keap1-Nrf2 axis modulation. The Nrf2 stabilization effect is direct as judged by the time-course of Neh2-luc reporter activation (*SI Appendix*, Fig. S8). To rule out the possibility that the stabilization of Nrf2 by HPPE in cellular models and in vivo (Fig. 5*C* and *SI Appendix*, Figs. S8 and S17*C*) is due to HPPE's ability to metabolize into active intermediates and byproducts, a simple assay was performed by incubating HPPE in the presence of human plasma in a test tube. This assay revealed no metabolites as judged by mass spectrometry (*SI Appendix*, Fig. S13). Hence, HPPE is highly stable and does not undergo chemical conversion in the presence of human plasma, meaning that HPPE works "as is" and stabilizes Nrf2. We speculate that HPPE can work as a zinc ionophore and target Zn-binding site in Keap1 to activate Nrf2 (40); however, this site is barely characterized, and its role in Keap1 function and stability is not known. Whatever the mechanism of Nrf2 stabilization by HPPE, this nonelectrophilic Bach1 inhibitor presents an exciting combination of the two activities necessary to trigger the antioxidant genetic program. Given the detailed characterization of the inhibitor properties, and especially in the absence of electrophilic properties, HPPE is perfectly suited for Bach1 pharmacological manipulation in vitro and in vivo.

HPPE Induces Genes Involved in Neuroprotective Pathways. The functional genomics analysis of gene expression data from Bach1 KO mice VMB revealed activation of various pathways that are involved in neuroprotection, neutralizing oxidative stress, and balancing cellular inflammatory environment (Fig. 3 and *SI Appendix*, Fig. S2 and Table S2). To evaluate whether similar pathways were triggered by HPPE, we performed gene expression analysis in N27 rat dopaminergic cells treated with HPPE. HPPE treatment resulted in significant up-regulation of both ARE and non–ARE-dependent genes (*SI Appendix*, Fig. S14*A*). Compared to the controls, ARE-dependent genes that were up-regulated by HPPE in N27 cells included *Hmox1*, *Gclc*, *Gclm*, *Nqo1*, *Mt3*, *Sod1*, and *Mt1*, whereas the non-ARE genes up-regulated by HPPE included *Hmox1*, *Neurod1*, and *Nr4a2* (*SI Appendix*, Fig. S14*A* and Table S5). Overall, HPPE treatment resulted in significant up-regulation of genes involved in heme degradation, redox regulation, cell cycle, negative regulation of neuronal apoptotic process, neuronal differentiation, protein homo-oligomerization, and subcellular transport processes (*SI Appendix*, Fig. S14*A*). To determine if the changes in the gene expression are reflected in the expression of their respective proteins, we evaluated protein expression of a subset of genes from cells treated with HPPE using immunoblot. We found an increased expression in *Hmox1*, *Nqo1*, *Gclc*, *Gclm*, and *Gsr* in N27 cells after HPPE treatment compared to controls (*SI Appendix*, Fig. S14 *B* and *C*). The change in expression of these proteins were long lasting, as the expressed proteins

stayed up-regulated until 48 h after HPPE exposure (*SI Appendix*, Fig. S14 *B* and *C*). Collectively, these results demonstrated that HPPE-mediated Bach1 inhibition resulted in efficient induction of both ARE- and non–ARE-mediated genes in vitro in rat dopaminergic N27 cells. To test expression of ARE and non-ARE genes in vivo, we performed pharmacokinetic analysis in mice following HPPE administration. Oral gavage of a single dose of HPPE (100 mg/kg body weight) in mice showed significant accumulation of HPPE in various tissues including liver, kidney, and brain. Levels of HPPE in all tissues peaked at 2 h after HPPE treatment which gradually declined by 24 h and were below the quantifiable level beyond 24 h (*SI Appendix*, Table S7). Gene expression analysis in the mouse VMB and STR at similar time points and dose used for pharmacokinetic analysis showed a marked increase in the expression of genes that were involved in heme degradation and redox regulatory processes including *Hmox1*, *Gsr*, *Mafg*, and *Me1* in both VMB and STR (*SI Appendix*, Fig. S14 *D* and *E*). In addition, a significant increase in the expression of *Prdx2*, *Txnip*, *Txnrd1*, and *Slc7a11* were observed in the VMB of HPPE-treated mice compared to vehicle control (*SI Appendix*, Fig. S14*D*). Most of the genes showed marked up-regulation in the VMB at 8 h after HPPE except for *Slc7a11* which was up-regulated at 2 h and *Txnrd1* up-regulated at 24 h. These results suggest that HPPE is orally active with an excellent pharmacokinetic profile and induces a battery of both ARE and non-ARE genes involved in neuroprotection, neutralizing oxidative stress, and balancing cellular inflammatory environment.

HPPE Ameliorates MPTP-Induced Dopaminergic Neurodegeneration and Associated Oxidative Stress and Neuroinflammation. To determine the impact of pharmacological inhibition of Bach1 in MPTP-induced dopaminergic cell death, we evaluated the effects of HPPE administration in an acute MPTP paradigm. Based on its pharmacokinetic profile in vivo (*SI Appendix*, Table S7), we treated HPPE twice a day by oral gavage. As displayed by the schematics in Fig. 7, HPPE was administered in pre- and posttreatment paradigms to determine neuroprotective effects against acute MPTP neurotoxicity. In the pretreatment paradigm, HPPE was administered twice daily for 3 d before MPTP injections and for the next 3 d after the last dose of MPTP. Stereological counts of SNpc dopaminergic neurons defined by TH and Nissl staining did not differ between vehicle and HPPE treatment (Fig. 7 *A* and *B*). SNpc dopaminergic neuronal counts were significantly reduced in the MPTP-treated group that received the vehicle (Fig. 7 *A* and *B*). However, SNpc dopaminergic neurons were significantly protected against MPTP neurotoxicity in the group treated with HPPE (5 and 10 mg/kg) in a dose-dependent manner, as more TH- and Nissl-stained SNpc neurons survived in HPPE groups compared to vehicle-treated MPTP mice (Fig. 7 *A* and *B*). Measurement of striatal levels of DA and its metabolites DOPAC and HVA did not differ between vehicle- and HPPE-treated groups (*SI Appendix*, Fig. S15*A*). Levels of DA and its metabolites were significantly reduced in MPTP-treated mice that received vehicle. However, in the HPPE-treated groups (5 and 10 mg/kg), MPTP-induced loss of DA and its metabolites was significantly attenuated compared to MPTP-injected mice that received the vehicle. To ascertain that resistance to MPTP neurotoxicity provided by HPPE was not because of alteration in the bioavailability of MPP+, we measured striatal levels of MPP+ 90 min after MPTP injection when pretreated with HPPE. Levels of MPP+ did not differ between MPTP-injected mice that received HPPE compared to those that received vehicle (*SI Appendix*, Table S8). These findings demonstrate that pretreatment of HPPE attenuates MPTP-induced dopaminergic

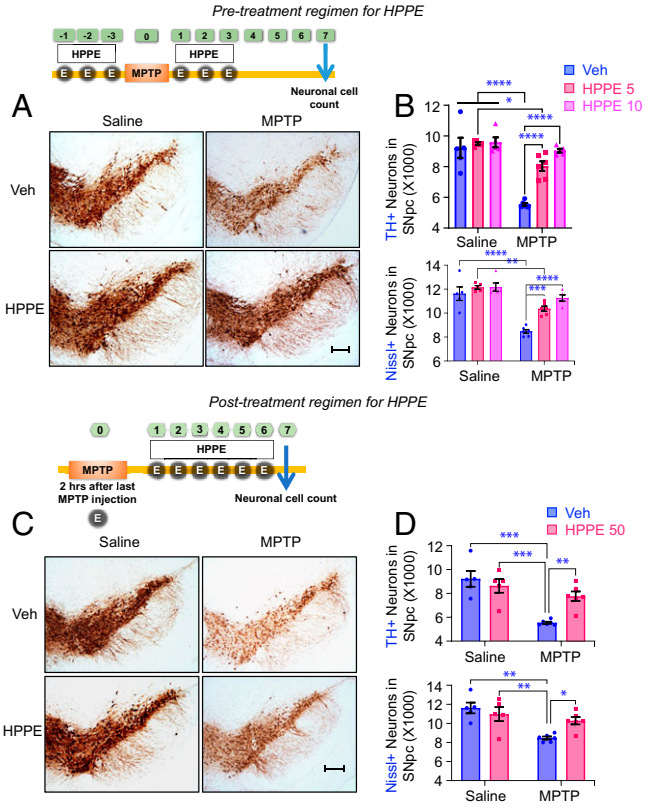

Fig. 7. Pre- and posttreatment of HPPE is neuroprotective against acute MPTP neurotoxicity. Schematic representation of timepoints for HPPE pretreatment in acute MPTP paradigm. (*A*) Immunohistochemical staining for TH in the SNpc of C57BL/6J mice on the seventh day following HPPE (5 and 10 mg/kg twice a day for 6 d by oral gavage) treatment in the acute MPTP model (MPTP.HCl 12 mg/kg, three injections 2 h apart) as explained in *Materials and Methods*. (Scale bar, 100 μm.) (*B*) Stereological analysis of total (Nissl) and TH+ neurons in the SNpc. Data expressed as mean ± SEM. One-way ANOVA with Tukey's multiple comparison was used to compare each treatment group (*$P < 0.05$, **$P < 0.005$, ***$P < 0.0005$, and ****$P < 0.0001$; $n = 5$ to 6). Schematic representation of timepoints for HPPE posttreatment in acute MPTP paradigm. (*C*) Immunohistochemical staining for TH in the SNpc of C57BL/6J mice on seventh day in the acute MPTP model (MPTP HCl 12 mg/kg, three injections 2 h apart) treated with HPPE (50 mg/kg twice a day for 6 d by oral gavage) 8 h after first dose of MPTP as explained in *Materials and Methods*. (Scale bar, 100 μm.) (*D*) Stereological analysis of total (Nissl) and TH+ neurons in the SNpc. Data expressed as mean ± SEM, One-way ANOVA followed by Tukey's multiple comparison (*$P < 0.05$, **$P < 0.005$, ***$P < 0.0005$, and ****$P < 0.0001$; $n = 5$ to 6).

neurotoxicity in mice without impacting the conversion of MPTP to MPP+ in the brain.

Given the neuroprotective effects of HPPE against MPTP neurotoxicity in the pretreatment regimen, we next determined its proficiency in the posttreatment paradigm. As shown in the schematics for the posttreatment regimen in Fig. 7*C*, HPPE was administered twice daily for 6 d after the last dose of MPTP in the acute paradigm, where the first dose of HPPE administered 8 h after the first dose of MPTP injection. Stereological counts of SNpc dopaminergic neurons defined by TH and Nissl staining showed no difference between groups treated with vehicle and HPPE (Fig. 7 *C* and *D*). SNpc dopaminergic neuronal counts were significantly reduced in the MPTP-treated group that received the vehicle (Fig. 7 *C* and *D*). However, SNpc dopaminergic neurons were significantly protected against MPTP neurotoxicity in the group that were treated with HPPE (50 mg/kg), as more TH- and Nissl-stained SNpc neurons survived in MPTP-treated mice administered with HPPE

compared to vehicle (Fig. 7 *C* and *D*). Measurement of striatal levels of DA and its metabolites DOPAC and HVA showed no difference between vehicle- and HPPE-treated groups (*SI Appendix*, Fig. S15*B*). Levels of DA and its metabolites were significantly reduced in MPTP-treated mice that received the vehicle. However, in mice administered with HPPE, MPTP-induced loss of DA and its metabolites were significantly attenuated compared to MPTP-injected mice that were administered with vehicle. These findings suggests that HPPE attenuates MPTP neurotoxicity when administered after MPTP injections in mice in a posttreatment paradigm.

To investigate if neuroprotective effects of HPPE against MPTP neurotoxicity are accompanied by reduction in markers of inflammation and oxidative stress, we evaluated the levels of 3-nitrotyrosine, CD68, and GFAP in the SNpc. Immunohistochemical analysis showed a significant increase in 3-NT immunoreactivity in the MPTP-injected mice compared to vehicle-treated mice (*SI Appendix*, Fig. S16*A*). Administration of HPPE significantly attenuated MPTP-induced increases in 3-NT immunoreactivity compared to mice injected with MPTP (*SI Appendix*, Fig. S16*A*). Quantitative analysis showed a marked increase in 3-NT–immunoreactive cells in MPTP-injected mice compared with vehicle-treated mice, which was significantly reduced in the MPTP-treated mice that received HPPE (*SI Appendix*, Fig. S16*B*). Similarly, MPTP administration significantly increased the CD68-immunopositive activated microglia (*SI Appendix*, Fig. S16*C*) and GFAP-immunopositive reactive astrocytes (*SI Appendix*, Fig. S16*E*) of MPTP-injected mice compared to vehicle-treated mice. HPPE treatment significantly attenuated levels of MPTP-induced reactive microglia and astrocytes compared to mice that received only MPTP. Morphometric analysis of CD68-positive reactive microglia and GFAP-positive reactive astrocytes in the SNpc showed a marked increase in the levels of reactive microglial and astrocytic cell counts in the MPTP-treated group compared with controls, which were markedly reduced in MPTP-treated mice that received HPPE (*SI Appendix*, Fig. S16 *D* and *F*). Consistent with the immunohistochemical markers of oxidative stress and neuroinflammation in the SNpc, mRNA analysis in the VMB of MPTP-injected mice demonstrated a significant increase in the levels of proinflammatory genes *TNF-α* and *Mcp-1* (*SI Appendix*, Fig. S17 *A* and *B*) and antioxidant gene *Nrf2* (*SI Appendix*, Fig. S17*C*). Administration of HPPE significantly reduced MPTP-induced increases in *TNF-α* and *Mcp-1* mRNA levels, and on the other hand, HPPE significantly increased mRNA levels of *Nrf2* compared to MPTP-treated mice that received the vehicle. Altogether, these findings suggest that neuroprotective effects of HPPE against MPTP neurotoxicity are associated with up-regulation of antioxidant genes, down-regulation of proinflammatory genes and reduction in markers of oxidative stress and inflammation.

Discussion

Numerous studies have suggested that Nrf2 activation can ameliorate neurodegeneration in preclinical models of PD (5, 41). Our findings reveal a previously unknown neuroprotective mechanism based on derepression of Bach1, a transcriptional inhibitor of the Nrf2 activity, in a mouse model of experimental PD. Several studies show a correlative decline in Nrf2 activity with age, which is a predominant risk factor for PD (42–44). However, in the SNpc dopaminergic neurons of PD patients from early Braak Stages I to II, Nrf2 was found in the nucleus, whereas it was localized to the cytosol in healthy age-matched controls (45). The translocation of Nrf2 to the nucleus in PD patients indicates an attempt to up-regulate Nrf2 target genes, the attempt that apparently fails to bring the Nrf2-driven genetic program to the level needed to fight against ongoing neurodegeneration in PD. The problem stems from an existent feedback regulation where continuous activation of Nrf2 is compensated by higher expression levels of Nrf2 transcriptional repressors (9). Notably, we observed up-regulation of Bach1 (a transcriptional repressor of Nrf2) protein levels in the SNpc of human PD patients and in animal and cellular models of PD (Fig. 1). Given that Bach1 is an Nrf2 target gene, an increase in Nrf2 protein stabilization is accompanied by a simultaneous increase in Bach1 expression, which will diminish the induction of Nrf2 target genes (9, 13, 42). Consistent with this viewpoint, we observed that Bach1-deficient mice were protected against MPTP neurotoxicity, associated oxidative damage, and neuroinflammation (Fig. 2 and *SI Appendix*, Figs. S1, S3, and S4). Our findings concur with reports of protective effects in Bach1-deficient mice against neuronal degeneration in spinal cord injury and experimental autoimmune encephalomyelitis (15, 16, 21). Functional genomic analysis suggest that Bach1-deficient mice were protected against MPTP due to up-regulation of both ARE and non-ARE (predominantly ETS motifs) genes (Fig. 3). Genes associated with Bach1-ARE motifs were enriched for pathways that were critical for oxygen sensing regulation and neuronal death, whereas genes enriched with non-ARE motifs were involved in DNA binding, inflammatory response, apoptosis, and neuronal death. Because Maf family of transcription factors heterodimerize with Bach1 (46) and ETS transcription factors during differentiation (47, 48) and immune response (49), Bach1 could essentially regulate non-ARE genes through ETS/MAF interactions. Taken together, our results suggest that Bach1 deficiency can up-regulate both Nrf2 genes and unexplored non-Nrf2 target genes which may have additional benefits against MPTP-neurotoxicity.

The Bach1 repression of its target genes is mediated by heterodimerization of Bach1 with small Maf proteins and its binding to Maf recognition element called MARE (11, 12). Bach1 derepression upon Bach1 binding to heme and porphyrin-like molecules is well studied and occurs through Bach1 multiple heme regulatory motifs (33). While heme/hemin is toxic (50, 51), metalloporphyrins are therapeutic in preclinical disease models associated with oxidative and nitrosative stress (52). However, metalloporphyrins have limited CNS bioavailability due to their poor blood–brain barrier penetration, so there is a strong need for a better drug candidate to pharmacologically inhibit Bach1. Drug screening performed with a proprietary translational technology platform coupled with MARE-luciferase reporter [WO 2012/094580 (31)] identified a substituted benzimidazole, HPPE, exhibiting an attractive combination of two desired activities which involves Bach1 inhibition (Fig. 4) and Nrf2 stabilization (Fig. 5*C* and *SI Appendix*, Fig. S8). HPPE demonstrated a micromolar half-activation constant compared to the FDA-approved Nrf2 activator, DMF, and physiological Bach1 inhibitor hemin, both working in 10- to 20-μM range (Fig. 4*B*). The specificity of HPPE for Bach1 heme-binding sites was verified by inhibition of HPPE-induced MARE-luciferase reporter activation when mutant Bach1 was overexpressed in the reporter cell line (Fig. 4*C*).

To confirm the nonalkylating nature of HPPE action in Bach1 inhibition and Nrf2 stabilization, we performed a thorough characterization of HPPE chemical properties. The results obtained proved HPPE nonalkylating nature with respect to free glutathione (Fig. 6*A*) and Keap1 thiols (*SI Appendix*, Fig. S10 *A* and *B*) and the absence of HPPE affinity for Keap1 Kelch domain in fluorescence polarization assay (*SI Appendix*, Fig. S10*D*). HPPE did not reduce the levels of GSH and increase ROS in neuronal cells (Fig. 6 *C* and *D*), and its activation in ARE-luciferase assay is not sensitive to high concentrations of cell-permeable reducing agent, NAC (Fig. 6 *E* and *F*), thus indicating the absence of oxidative transformation of HPPE in the cell.

Analysis of physical binding of HPPE to recombinant Bach1 using mass spectrometry showed that HPPE was unable to covalently modify Bach1 cysteines whereas DMF treatment resulted in nonenzymatic succination of Bach1 cysteines (*SI Appendix*, Table S6), consistent with reports on DMF-modified active cysteines in proteins affecting various cellular pathways resulting in side-effects (53, 54). Thus, even though HPPE and DMF both activate MARE-luciferase reporter (Fig. 4*B*), they work by entirely different mechanisms. HPPE has been confirmed as a nonelectrophile and its likely mechanism of action is based on noncovalent Bach1 binding. Since overexpression of mutated Bach1, with cysteines in heme-binding CP motifs replaced by alanine, completely inhibited MARE-luciferase activation by HPPE as well as by Co-PPIX (Fig. 4*C*), the mechanism of HPPE action on Bach1 likely includes modulation of the heme-binding regulatory motifs, in a fashion similar to Co-PPIX and hemin (32). The structural similarity between HPPE and porphyrin (i.e., HPPE resembles one-half of the porphyrin ring) suggests that HPPE will act similar to hemin. However, HPPE is a not an iron chelator, since the two potential ligands in HPPE molecule are located on separate and freely rotating moieties, and therefore HPPE will not exert any pro-oxidant activity and toxicity like hemin, where the iron is 4-coordinated by porphyrin ring pyrroles and behaves as a catalyst for oxygen/hydrogen peroxide activation and lipid peroxidation (51, 55). The confirmed absence of HPPE alkylating potency with respect to both Keap1 and Bach1 supports HPPE classification as a true Bach1 inhibitor, free of deleterious effects as those of hemin but working at the heme-binding sites of Bach1 protein.

Bach1 derepression should include at least two steps—Bach1 dissociation from the DNA binding element followed by its nuclear export. We performed the nuclear export inhibition experiment for HPPE-induced Hmox1 up-regulation (Fig. 5 *A*–*C*) similarly to the hemin-mediated experiment described by Suzuki and colleagues (35). In the presence of Crm1-dependent nuclear export inhibitor leptomycin B, HPPE-induced Hmox1 up-regulation was blocked (Fig. 5*A*), and Bach1 protein content in the nucleus was higher in the nucleus and lower in the cytosolic fraction when compared to HPPE alone (Fig. 5*C*). Hence HPPE, similar to hemin, supports Bach1 nuclear export. An inhibition of HPPE-induced Hmox1 up-regulation in the presence of leptomycin B was observed despite the significant accumulation of Nrf2 in the nucleus. This observation justifies the need in Bach1 inhibition to fully explore the benefits of Nrf2 stabilization. Nevertheless, our ChIP assays showed that similar to hemin, HPPE treatment results in ca. 10-fold drop in Bach1 occupancy on EN1 and EN2 enhancer regions of Hmox1 promoter with the corresponding rise in Nrf2 occupancy at the same regions (Fig. 5 *D* and *E* and *SI Appendix*, Fig. S7). Altogether, our studies recommend HPPE as a benign mimic of hemin and promising drug candidate to manipulate Bach1.

Both in vitro and in vivo studies demonstrated that HPPE treatment up-regulated gene signatures that were similar to those observed in the brains of Bach1 KO mice (*SI Appendix*, Fig. S14*A*), which included both ARE-dependent and ARE-independent cellular pathways (*SI Appendix*, Fig. S19). Our experimental results showed that oral administration of HPPE was safe, well-tolerated, and ameliorated MPTP-induced nigrostriatal dopaminergic neurodegeneration in a pretreatment and, most importantly, in a posttreatment paradigm, where majority of Nrf2 activators show no benefit at all. MPTP treatment in mice results in marked increases in oxidative damage, glial activation, and levels of proinflammatory cytokines, resulting in dopaminergic neurodegeneration. Postmortem human PD brains accumulate elevated levels of oxidative stress markers such as oxidized proteins, lipids, and nucleic acids and abnormally activated glia that secrete toxic cytokines (30). HPPE treatment significantly blocked accumulation of oxidative stress marker 3-nitrotyrosine, numbers of reactive microglia and astrocytes in the SNpc, and increases in proinflammatory genes and a corresponding increase in neuroprotective genes suggesting that Bach1 inhibition is beneficial in blocking oxidative stress and neuroinflammation associated with MPTP neurotoxicity (*SI Appendix*, Figs. S16 and S17). We demonstrated that orally active nonelectrophilic Bach1 inhibitor HPPE up-regulates Bach1-dependent ARE and non-ARE gene signatures with robust neuroprotective properties in a posttreatment mouse model of PD. Among the neuroprotective genes, Bach1 inhibition resulted in increased expression of genes such as *Gclm*, *Gclc*, *Gsr*, and *Slc7a11* (*SI Appendix*, Fig. S14), which are crucial in mitigating neurodegeneration caused by ferroptosis (56). These findings are consistent with a recent study showing Bach1 ablation can protect against ferroptosis in a myocardial infarction model (22). Given the significant similarity in bZIP domains of Bach1 and Bach2 (57) and the fact that heme can serve as a ligand for Bach2 (58), HPPE administration in mice resulted in a modest but significant up-regulation of mRNA levels of *Bach2* and its target gene B lymphocyte–induced maturation protein-1 (*Blimp1)* in the VMB (*SI Appendix*, Fig. S18*A*). However, in the Bach1 KO mice, mRNA levels of *Bach2* and *Blimp1* in the VMB were not significantly different compared to WT mice (*SI Appendix*, Fig. S18*B*). Hence, Bach1 inhibition/genetic deletion is sufficient to provide the observed neuroprotection in the MPTP model. Our studies further support the evaluation of HPPE in chronic models of PD to gain additional insights into how Bach1 inhibitors protect against neurodegeneration and their use in clinical trials to treat PD. Future studies should also investigate HPPE's role in the expression of Bach2 target genes in various organs and cellular systems to determine their influence in normal physiology and in pathophysiological conditions. In summary, the mechanism of pharmacological action of HPPE involved a favorable combination of Nrf2 stabilization and Bach1 inhibition, which resolves the feedback regulation issue resulting in Bach1 upregulation due to Nrf2 activation. Nonelectrophilic displacement Nrf2 activators, as of today, lose the battle to alkylating Nrf2 activators, which are more efficient in vivo despite their unavoidable "accumulated" toxicity/side effects. However, for conditions like PD and other forms of chronic neurodegeneration, nonelectrophilic Bach1 inhibitors and nonelectrophilic Nrf2 displacement activators combined in one molecule is a promising therapeutic strategy to restore homeostatic redox balance.

Materials and Methods

Human Postmortem Brains. Postmortem substantia nigra from subjects with an antemortem clinical diagnosis of PD (n = 9) and age-matched controls (n = 5) were obtained from Johns Hopkins University and University of Maryland Brain and Tissue Bank, Baltimore. PD patients and control subjects from both sexes did not differ significantly in their mean age at death (controls 76 ± 7 y; PD patients, 78 ± 6) (*SI Appendix*, Table S1). All participants agreed to a detailed clinical evaluation and brain donation upon their death.

Additional details of reagents and methods are provided in *SI Appendix*.

Data Availability. Microarray data have been deposited in the Gene Expression Omnibus (GSE164412). All other study data are included in the article and/or *SI Appendix*.

ACKNOWLEDGMENTS. This work was supported by the NIH Grant Nos. NS101967 and S10 OD025126, Michael J. Fox Foundation for Parkinson's disease, Parkinson Foundation, PAR Fore Parkinson, Russian Scientific Foundation Grant No. 20-15-00207, and Higher School of Economics University Basic Research Program. This work made use of the Integrated Molecular Structure Education and Research Center at Northwestern University, which received support from the Soft and Hybrid Nanotechnology Experimental Resource (NSF ECCS-1542205), the State of Illinois, and the International Institute for Nanotechnology. We are grateful to Prof. Terrance Kavanagh (University of Washington) for GCLC and GCLM antibodies, Prof. Curt Freed (University of Colorado) for rat dopaminergic 1RB3AN27 (N27) cells, Prof. Roland Wolf

(University of Dundee) for AREc32 cells, and Johns Hopkins University and University of Maryland for postmortem human brain tissue. We acknowledge the assistance of Jennifer R. Bethard (Medical University of South Carolina) and Wenbo Zhi (Augusta University) for mass spectrometry analysis.

1. B. R. Bloem, M. S. Okun, C. Klein, Parkinson's disease. *Lancet* **397**, 2284–2303 (2021).
2. D. K. Simon, C. M. Tanner, P. Brundin, Parkinson disease epidemiology, pathology, genetics, and pathophysiology. *Clin. Geriatr. Med.* **36**, 1–12 (2020).
3. GBD 2016 Parkinson's Disease Collaborators, Global, regional, and national burden of Parkinson's disease, 1990-2016: A systematic analysis for the Global Burden of Disease Study 2016. *Lancet Neurol.* **17**, 939–953 (2018).
4. E. R. Dorsey, T. Sherer, M. S. Okun, B. R. Bloem, The emerging evidence of the Parkinson pandemic. *J. Parkinsons Dis.* **8**, S3–S8 (2018).
5. N. Ammal Kaidery, M. Ahuja, B. Thomas, Crosstalk between Nrf2 signaling and mitochondrial function in Parkinson's disease. *Mol. Cell. Neurosci.* **101**, 103413 (2019).
6. L. Baird, M. Yamamoto, The molecular mechanisms regulating the KEAP1-NRF2 pathway. *Mol. Cell. Biol.* **40**, e00099-20 (2020).
7. F. Katsuoka *et al.*, Genetic evidence that small maf proteins are essential for the activation of antioxidant response element-dependent genes. *Mol. Cell. Biol.* **25**, 8044–8051 (2005).
8. M. P. Hoffman, T. W. Cutress, S. Tomiki, Prevalence of developmental defects of enamel in children in the Kingdom of Tonga. *N. Z. Dent. J.* **84**, 7–10 (1988).
9. D. M. Hushpulian *et al.*, Challenges and limitations of targeting the Keap1-Nrf2 pathway for neurotherapeutics: Bach1 de-repression to the rescue. *Front. Aging Neurosci.* **13**, 673205 (2021).
10. I. G. Gazaryan, B. Thomas, The status of Nrf2-based therapeutics: Current perspectives and future prospects. *Neural Regen. Res.* **11**, 1708–1711 (2016).
11. K. Igarashi, J. Sun, The heme-Bach1 pathway in the regulation of oxidative stress response and erythroid differentiation. *Antioxid. Redox Signal.* **8**, 107–118 (2006).
12. T. Oyake *et al.*, Bach proteins belong to a novel family of BTB-basic leucine zipper transcription factors that interact with MafK and regulate transcription through the NF-E2 site. *Mol. Cell. Biol.* **16**, 6083–6095 (1996).
13. X. Zhang *et al.*, Bach1: Function, regulation, and involvement in disease. *Oxid. Med. Cell. Longev.* **2018**, 1347969 (2018).
14. J. Lee *et al.*, Effective breast cancer combination therapy targeting BACH1 and mitochondrial metabolism. *Nature* **568**, 254–258 (2019).
15. H. Kanno *et al.*, Genetic ablation of transcription repressor Bach1 reduces neural tissue damage and improves locomotor function after spinal cord injury in mice. *J. Neurotrauma* **26**, 31–39 (2009).
16. K. Yamada *et al.*, Modulation of the secondary injury process after spinal cord injury in Bach1-deficient mice by heme oxygenase-1. *J. Neurosurg. Spine* **9**, 611–620 (2008).
17. Y. Watari *et al.*, Ablation of the bach1 gene leads to the suppression of atherosclerosis in bach1 and apolipoprotein E double knockout mice. *Hypertens. Res.* **31**, 783–792 (2008).
18. S. Yu, J. Zhai, J. Yu, Q. Yang, J. Yang, Downregulation of BACH1 protects against cerebral ischemia/reperfusion injury through the functions of HO-1 and NQO1. *Neuroscience* **436**, 154–166 (2020).
19. Y. Liu *et al.*, BTB and CNC homology 1 inhibition ameliorates fibrosis and inflammation via blocking ERK pathway in pulmonary fibrosis. *Exp. Lung Res.* **47**, 67–77 (2021).
20. L. Casares *et al.*, Isomeric O-methyl cannabidiolquinones with dual BACH1/NRF2 activity. *Redox Biol.* **37**, 101689 (2020).
21. A. Y. So *et al.*, Regulation of APC development, immune response, and autoimmunity by Bach1/HO-1 pathway in mice. *Blood* **120**, 2428–2437 (2012).
22. H. Nishizawa *et al.*, Ferroptosis is controlled by the coordinated transcriptional regulation of glutathione and labile iron metabolism by the transcription factor BACH1. *J. Biol. Chem.* **295**, 69–82 (2020).
23. N. M. Anderson, M. C. Simon, BACH1 orchestrates lung cancer metastasis. *Cell* **178**, 265–267 (2019).
24. N. Shajari *et al.*, Silencing of BACH1 inhibits invasion and migration of prostate cancer cells by altering metastasis-related gene expression. *Artif. Cells Nanomed. Biotechnol.* **46**, 1495–1504 (2018).
25. S. Davudian, B. Mansoori, N. Shajari, A. Mohammadi, B. Baradaran, BACH1, the master regulator gene: A novel candidate target for cancer therapy. *Gene* **588**, 30–37 (2016).
26. V. Jackson-Lewis, M. Jakowec, R. E. Burke, S. Przedborski, Time course and morphology of dopaminergic neuronal death caused by the neurotoxin 1-methyl-4-phenyl-1,2,3,6-tetrahydropyridine. *Neurodegeneration* **4**, 257–269 (1995).
27. R. Ebina-Shibuya *et al.*, The double knockout of Bach1 and Bach2 in mice reveals shared compensatory mechanisms in regulating alveolar macrophage function and lung surfactant homeostasis. *J. Biochem.* **160**, 333–344 (2016).
28. A. Subramanian *et al.*, Gene set enrichment analysis: A knowledge-based approach for interpreting genome-wide expression profiles. *Proc. Natl. Acad. Sci. U.S.A.* **102**, 15545–15550 (2005).
29. J. M. Taylor, B. S. Main, P. J. Crack, Neuroinflammation and oxidative stress: Co-conspirators in the pathology of Parkinson's disease. *Neurochem. Int.* **62**, 803–819 (2013).
30. B. Thomas, Parkinson's disease: From molecular pathways in disease to therapeutic approaches. *Antioxid. Redox Signal.* **11**, 2077–2082 (2009).
31. O. C. Attucks *et al.*, Induction of heme oxygenase I (HMOX1) by HPP-4382: A novel modulator of Bach1 activity. *PLoS One* **9**, e101044 (2014).
32. Y. Zenke-Kawasaki *et al.*, Heme induces ubiquitination and degradation of the transcription factor Bach1. *Mol. Cell. Biol.* **27**, 6962–6971 (2007).
33. K. Ogawa *et al.*, Heme mediates derepression of Maf recognition element through direct binding to transcription repressor Bach1. *EMBO J.* **20**, 2835–2843 (2001).
34. Y. Shan, R. W. Lambrecht, S. E. Donohue, H. L. Bonkovsky, Role of Bach1 and Nrf2 in up-regulation of the heme oxygenase-1 gene by cobalt protoporphyrin. *FASEB J.* **20**, 2651–2653 (2006).
35. H. Suzuki *et al.*, Heme regulates gene expression by triggering Crm1-dependent nuclear export of Bach1. *EMBO J.* **23**, 2544–2553 (2004).
36. H. Suzuki *et al.*, Cadmium induces nuclear export of Bach1, a transcriptional repressor of heme oxygenase-1 gene. *J. Biol. Chem.* **278**, 49246–49253 (2003).
37. M. Ahuja *et al.*, Distinct Nrf2 signaling mechanisms of fumaric acid esters and their role in neuroprotection against 1-methyl-4-phenyl-1,2,3,6-tetrahydropyridine-induced experimental Parkinson's-like disease. *J. Neurosci.* **36**, 6332–6351 (2016).
38. R. A. Linker *et al.*, Fumaric acid esters exert neuroprotective effects in neuroinflammation via activation of the Nrf2 antioxidant pathway. *Brain* **134**, 678–692 (2011).
39. M. S. Brennan *et al.*, Dimethyl fumarate and monoethyl fumarate exhibit differential effects on KEAP1, NRF2 activation, and glutathione depletion in vitro. *PLoS One* **10**, e0120254 (2015).
40. M. McMahon, S. R. Swift, J. D. Hayes, Zinc-binding triggers a conformational-switch in the cullin-3 substrate adaptor protein KEAP1 that controls transcription factor NRF2. *Toxicol. Appl. Pharmacol.* **360**, 45–57 (2018).
41. D. A. Johnson, J. A. Johnson, Nrf2–A therapeutic target for the treatment of neurodegenerative diseases. *Free Radic. Biol. Med.* **88**, 253–267 (2015).
42. L. Zhou, H. Zhang, K. J. A. Davies, H. J. Forman, Aging-related decline in the induction of Nrf2-regulated antioxidant genes in human bronchial epithelial cells. *Redox Biol.* **14**, 35–40 (2018).
43. J. H. Suh *et al.*, Decline in transcriptional activity of Nrf2 causes age-related loss of glutathione synthesis, which is reversible with lipoic acid. *Proc. Natl. Acad. Sci. U.S.A.* **101**, 3381–3386 (2004).
44. T. J. Collier, N. M. Kanaan, J. H. Kordower, Ageing as a primary risk factor for Parkinson's disease: Evidence from studies of non-human primates. *Nat. Rev. Neurosci.* **12**, 359–366 (2011).
45. C. P. Ramsey *et al.*, Expression of Nrf2 in neurodegenerative diseases. *J. Neuropathol. Exp. Neurol.* **66**, 75–85 (2007).
46. J. Sun *et al.*, Heme regulates the dynamic exchange of Bach1 and NF-E2-related factors in the Maf transcription factor network. *Proc. Natl. Acad. Sci. U.S.A.* **101**, 1461–1466 (2004).
47. M. H. Sieweke, H. Tekotte, J. Frampton, T. Graf, MafB is an interaction partner and repressor of Ets-1 that inhibits erythroid differentiation. *Cell* **85**, 49–60 (1996).
48. Y. Bakri *et al.*, Balance of MafB and PU.1 specifies alternative macrophage or dendritic cell fate. *Blood* **105**, 2707–2716 (2005).
49. D. Aschenbrenner *et al.*, An immunoregulatory and tissue-residency program modulated by c-MAF in human T_H17 cells. *Nat. Immunol.* **19**, 1126–1136 (2018).
50. L. Goldstein, Z. P. Teng, E. Zeserson, M. Patel, R. F. Regan, Hemin induces an iron-dependent, oxidative injury to human neuron-like cells. *J. Neurosci. Res.* **73**, 113–121 (2003).
51. D. Chiabrando, F. Vinchi, V. Fiorito, S. Mercurio, E. Tolosano, Heme in pathophysiology: A matter of scavenging, metabolism and trafficking across cell membranes. *Front. Pharmacol.* **5**, 61 (2014).
52. H. Sheng *et al.*, Metalloporphyrins as therapeutic catalytic oxidoreductants in central nervous system disorders. *Antioxid. Redox Signal.* **20**, 2437–2464 (2014).
53. F. Humphries *et al.*, Succination inactivates gasdermin D and blocks pyroptosis. *Science* **369**, 1633–1637 (2020).
54. M. D. Kornberg *et al.*, Dimethyl fumarate targets GAPDH and aerobic glycolysis to modulate immunity. *Science* **360**, 449–453 (2018).
55. S. R. Robinson, T. N. Dang, R. Dringen, G. M. Bishop, Hemin toxicity: A preventable source of brain damage following hemorrhagic stroke. *Redox Rep.* **14**, 228–235 (2009).
56. S. J. Guiney, P. A. Adlard, A. I. Bush, D. I. Finkelstein, S. Ayton, Ferroptosis and cell death mechanisms in Parkinson's disease. *Neurochem. Int.* **104**, 34–48 (2017).
57. Y. Zhou, H. Wu, M. Zhao, C. Chang, Q. Lu, The bach family of transcription factors: A comprehensive review. *Clin. Rev. Allergy Immunol.* **50**, 345–356 (2016).
58. M. Watanabe-Matsui *et al.*, Heme regulates B-cell differentiation, antibody class switch, and heme oxygenase-1 expression in B cells as a ligand of Bach2. *Blood* **117**, 5438–5448 (2011).